

# Residual velocities of Small Magellanic Cloud star clusters

Andrés E. Piatti<sup>1,2\*</sup>

<sup>1</sup>*Instituto Interdisciplinario de Ciencias Básicas (ICB), CONICET-UNCUYO, Padre J. Contreras 1300, M5502JMA, Mendoza, Argentina*

<sup>2</sup>*Consejo Nacional de Investigaciones Científicas y Técnicas, Godoy Cruz 2290, C1425FQB, Buenos Aires, Argentina*

Accepted XXX. Received YYY; in original form ZZZ

## ABSTRACT

We analyzed the largest Small Magellanic Cloud (SMC) cluster sample (32) with proper motions and radial velocity measurements, from which we obtained their space velocity components. By adopting as a reference the recent best-fitted rotating disc of SMC star clusters as a function of the position angle, we computed their residual velocity vectors, and compared their magnitudes ( $\Delta V$ ) with that of a cluster with residual velocity components equal to the velocity dispersions along the three independent SMC rotating disc axes of motion ( $\Delta V = 60$  km/s). We found that clusters that belong to SMC tidally induced structures have  $\Delta V > 50$  km/s, which suggests that space velocities of clusters in the process of escaping the rotating disc kinematics, are measurably different. Studied clusters pertaining to a northern branch of the Magellanic Bridge, the main Magellanic Bridge, the Counter-Bridge and the West halo give support to these findings. NGC 121, the oldest known SMC cluster, does not belong to any SMC tidal feature, and has  $\Delta V = 64$  km/s, slightly above the boundary between bound and kinematically perturbed clusters.

**Key words:** galaxies: individual: SMC – galaxies: star clusters: general

## 1 INTRODUCTION

Recently, Piatti (2021a) obtained a rotating disc for Small Magellanic Cloud (SMC) star clusters using available radial velocities, derived proper motions, and positions of 25 clusters with ages between  $\sim 1$  and 10 Gyr old. He computed the three rotational velocity components (van der Marel et al. 2002) of each cluster for  $5.3 \times 10^8$  possible combinations of values of right ascension and declination of its centre, of heliocentric distance of its centre, of radial velocity and proper motions in right ascension and declination, of inclination of the disc, of position angle of the line-of-nodes, of rotational velocity, and of velocity dispersions along the three independent axes of motion. The resulting rotating disc, represented by a combination of parameter values that best resembled the observed clusters' movements, turned out to be very similar to that best-fitted by Zivick et al. (2020) for field SMC giants (see, also Niederhofer et al. 2021; De Leo et al. 2020; Gaia Collaboration et al. 2020). This means that both galaxy components are kinematically synchronized at some level for distances smaller than  $\sim 2$  kpc from the SMC centre.

The SMC clusters' motions derived by Piatti (2021a) show also some noticeable scatter around the obtained representative rotating disc, which is not caused by the considerable range of the clusters' ages used. Instead, Piatti (2021a) found that the velocity dispersion plays an important role in dealing with such a scatter around the mean rotation curve. Particularly, he found that velocity dispersions of 50, 20, and 25 km/s along the right ascension, declination, and line-of-sight axes, respectively, reasonably represent the observed velocity dispersion. This finding reveals that a rotating disc is not enough to describe the SMC clusters' kinematics and therefore, there exists clusters with motions that depart from that of the rotation on a plane around the SMC centre. According to Piatti (2021a), the rotating disc is roughly a tilted edge-on disc (disc inclination =  $(70.0 \pm 10.0)^\circ$ , position angle of the line-of-nodes =  $(200.0 \pm 30.0)^\circ$ ), with a stretching along the direction perpendicular to it, that nearly coincides with that of the Magellanic Clouds connecting bridge.

It has been shown that the SMC is under tidal effects by the interaction with the Large Magellanic Cloud (LMC, Pieres et al. 2017; Zivick et al. 2018; Mackey et al. 2018; De Leo et al. 2020; Niederhofer et al. 2021; Omkumar et al. 2021). Besla et al. (2012) showed that the observed irregular morphology and internal kinematics of the Magellanic System (in gas and stars) are naturally explained by interactions between the LMC and SMC, rather than gravitational interactions with the Milky Way. They examined the

\* E-mail: andres.piatti@unc.edu.ar

gas and stellar kinematic centres of the LMC; the warped LMC old stellar disc and bar; the gaseous arms stripped out of the LMC by the SMC in the direction of the Magellanic Bridge; the stellar debris from the SMC seen in the LMC disc field; etc., to strongly reinforce the suspicions of [de Vaucouleurs & Freeman \(1972\)](#) that the interaction with the Milky Way is not responsible for the LMC/SMC's morphology. Moreover, these conclusions provide further support that the Magellanic Clouds are completing their first infall to the Milky Way. Hence, a question arises unavoidably: Are SMC tidal structures kinematically different from that of the SMC rotating disc? or in other words, do kinematically perturbed clusters have any kinematic signatures that differentiate them from bound clusters? [Dias et al. \(2021\)](#) observed clusters located in a branch of the Magellanic Bridge, placed toward the northeastern outskirts of the SMC; in the SMC main body; and in the so-called Counter-Bridge, that is nearly superimpose in the sky to that Magellanic Bridge branch. They estimated heliocentric distances, radial velocities, and proper motions for a sample of 7 clusters that can be useful, once they are converted into space velocity components, to probe the existence of any distinguishable kinematic features between clusters belonging to these three different galaxy structures, two of them (Magellanic Bridge and Counter-Bridge) originated by tidal interaction with the LMC ([Dias & Bekki 2012](#); [Besla et al. 2016](#)).

In this work, we show that there exist different space residual velocities for clusters that are spatially distributed throughout SMC tidal structures and those bound to the SMC main body. This outcome allowed us to propose a simple kinematic criterion to assess at first glance whether a SMC cluster is bound to the galaxy or belong to any kinematically perturbed stellar component. In Section 2 we describe the gathered data employed in this work, while in Section 3 we analyze and discuss the kinematic characteristics of SMC clusters distributed at projected distances in the sky between  $\sim 1$  kpc and 4 kpc from the SMC centre.

## 2 DATA GATHERING

We used the  $v_1$ ,  $v_2$ , and  $v_3$  space velocity components according to [van der Marel et al. \(2002\)](#) of 25 SMC clusters analyzed by [Piatti \(2021a\)](#) and those of the 7 clusters studied by [Dias et al. \(2021\)](#). As far as we are aware, this is the largest sample of SMC clusters with derived space velocity components. They were calculated from measured radial velocities and proper motions, and the transformation equations (9), (13), and (21) in [van der Marel et al. \(2002\)](#) (see, also [Piatti et al. 2019](#)). We started from the hypothesis of, if a cluster has been perturbed by the LMC, its circular motion should change, and in the process of escaping from the SMC, its velocity behavior will be measurably different. In order to avoid projection effects of the clusters' motions space velocity components are suitable; inspecting proper motions or radial velocities could be misleading.

We also searched the literature for accurate heliocentric distances of the cluster sample. Unfortunately, only the 7 clusters studied by [Dias et al. \(2021\)](#) (B 168, BS 188, BS 196, HW 56, HW 85, IC 1708, L1) and 12 clusters analyzed by [Piatti \(2021a\)](#) (K 1, K 3, K 4, K 8, K 44, L 1, L 110, L 113, NGC 121, NGC 339, NGC 361, NGC 419) have available dis-

tances. Their values and corresponding uncertainties were taken from [Crowl et al. \(2001\)](#); [Glatt et al. \(2008\)](#); [Dias et al. \(2016\)](#); [Parisi et al. \(2014\)](#); [Martínez-Vázquez et al. \(2021\)](#); and [Dias et al. \(2021\)](#). We also computed the position angles of the clusters from north to east. Table 1 lists the values of position angles and distances adopted, alongside with their respective references.

From a careful reading of the references used to compile SMC clusters' distances, it turns out to be that the estimation of distances of SMC clusters has not been targeted by any observational campaign yet. On the contrary, there is a very limited number of SMC clusters with distance measurements. Most of them have been obtained from Padova's isochrone fitting using very sophisticated statistical methods (see, e.g. [Dias et al. 2016, 2021](#)) and/or considering spectroscopic metallicities (see, e.g. [Glatt et al. 2008](#); [Parisi et al. 2014](#); [Dias et al. 2021](#)). The compiled distances are the most valuable treasure available up-to-date to carry out the analysis described in Section 3, whose results must be interpreted as those based on the available cluster sample. The outcomes found in this work are pioneers to uncover an SMC picture that allows us to question about the nature and consequences of the interactions between both Magellanic Clouds. Precisely, this pioneering approach anticipates further studies that will be hopefully carried out from observational data obtained from the new generation telescopes.

Table 1 indicates the method employed to estimate the adopted distances, namely: theoretical isochrone fits to the cluster colour-magnitude diagrams, magnitudes of the cluster red giant clumps, or the Luminosity-Period relationship for  $\delta$  Sct stars. We adopted here as a reference distance scale that of the Padova theoretical isochrones ([Bressan et al. 2012](#)), because  $\sim 65\%$  of the cluster sample have distance estimates that rely on those isochrones. Using 7 clusters in our sample with distances estimated from fitting of Teramo ([Pietrinferni et al. 2004](#)) and Dartmouth ([Dotter et al. 2007](#)) isochrones, we found a mean difference in the distance modulus of (Teramo - Dartmouth) of  $0.009 \pm 0.021$  mag, and for 4 clusters in common in our sample with distances from Padova and Teramo isochrone fits, a difference in the distance modulus of  $-0.008 \pm 0.020$  mag. We note that a difference of 0.01 mag in the distance modulus implies a distance difference of 0.27 kpc at a distance of 60 kpc. Therefore, we assumed that there is no offsets between distances obtained from these sets of theoretical isochrones that could affect the subsequent analysis. As for distances derived from estimation of the magnitude of the Red Clump, we found 4 clusters (K 3, L 1, NGC 121, 339; [Crowl et al. 2001](#)) with distances estimated using the Red Clump method and Padova isochrone fits (see Table 1) and the mean difference turned out to be (Red Clump - Padova iso) =  $-2.5 \pm 1.2$  kpc. Therefore, we corrected the distances of K 44, L 113 and NGC 361 by adding 2.5 kpc to the mean values listed in Table 1. As for the distance of NGC 419, we found a mean difference of 0.1 kpc with respect to the value estimated from Padova isochrone fits ([Glatt et al. 2008](#)).

## 3 ANALYSIS AND DISCUSSION

The rotating disc geometry obtained by [Piatti \(2021a\)](#), see his Fig. 4) can be described as a 3D vector with components

**Table 1.** Properties of SMC star clusters.

| ID       | PA (deg) | $\Delta V$ (km/s) | $D$ (kpc) | Method                         | Ref. |
|----------|----------|-------------------|-----------|--------------------------------|------|
| Bruck168 | 50.8     | 29.2±49.4         | 61.9±2.1  | Padova iso                     | 6    |
| BS188    | 67.9     | 115.7±40.5        | 52.7±3.0  | Padova iso                     | 6    |
| BS196    | 56.9     | 80.6±35.7         | 50.1±2.0  | Padova iso                     | 6    |
| HW56     | 30.3     | 63.8±40.0         | 53.5±1.2  | Padova iso                     | 6    |
| HW85     | 65.6     | 112.1±44.0        | 54.0±1.6  | Padova iso                     | 6    |
| IC1708   | 54.0     | 145.5±48.5        | 65.2±1.5  | Padova iso                     | 6    |
| K1       | 247.2    | 73.1±34.2         | 53.7±2.4  | Teramo & Dartmouth iso         | 4    |
| K3       | 270.9    | 14.6±27.0         | 60.6±1.1  | Padova, Teramo & Dartmouth iso | 2    |
| K4       | 248.0    | 24.4±37.2         | 54.9±2.3  | Teramo & Dartmouth iso         | 4    |
| K8       | 255.0    | 99.2±24.0         | 69.8±2.3  | Padova iso                     | 3    |
| K44      | 149.5    | 48.0±32.2         | 62.2±2.7  | Red Clump                      | 1    |
| L1       | 259.5    | 129.2±20.7        | 56.9±1.0  | Padova, Teramo & Dartmouth iso | 2    |
| L100     | 61.4     | 78.1±36.3         | 58.6±0.7  | Padova iso                     | 6    |
| L110     | 90.8     | 58.2±32.7         | 47.9±2.3  | Teramo & Dartmouth             | 4    |
| L113     | 102.7    | 98.8±33.2         | 50.5±1.7  | Red Clump                      | 1    |
| NGC121   | 302.2    | 63.6±25.9         | 64.9±1.2  | Padova, Teramo & Dartmouth iso | 2    |
| NGC339   | 168.9    | 42.0±29.7         | 57.6±4.1  | Padova, Teramo & Dartmouth iso | 2    |
| NGC361   | 31.3     | 44.2±16.9         | 55.8±1.7  | Red Clump                      | 1    |
| NGC419   | 92.7     | 44.6±21.2         | 56.2±1.3  | $\delta$ Sct L-P relation      | 5    |

Ref.: (1) [Crowl et al. \(2001\)](#); (2) [Glatt et al. \(2008\)](#); (3) [Dias et al. \(2016\)](#); (4) [Parisi et al. \(2014\)](#); (5) [Martínez-Vázquez et al. \(2021\)](#); (6) [Dias et al. \(2021\)](#).

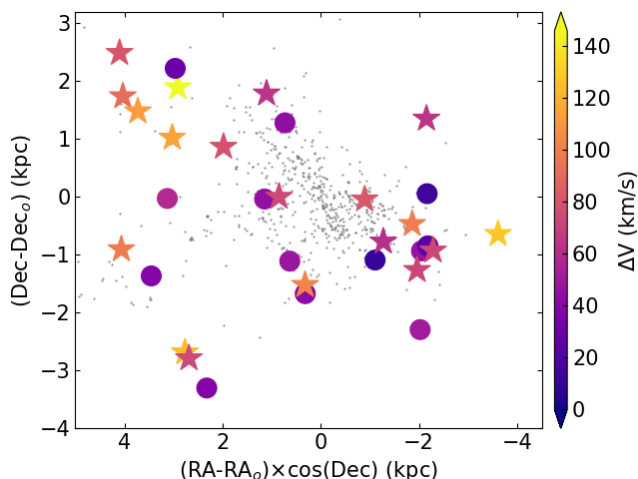


**Figure 1.** Spatial distribution of SMC clusters compiled in [Bica et al. \(2020\)](#) (gray dots). Coloured circles and stars correspond to clusters with residual velocities smaller and larger than 60 km/s.

$v_1$ ,  $v_2$ , and  $v_3$  that are functions of the position angle (PA). Therefore, the differences between each velocity component of a cluster and the respective ones for the rotational curve at the cluster’s PA ( $\Delta v_i$ ,  $i=1,2,3$ ) represent the components of the residual velocity vector with respect to the SMC rotating disc. By adding them in quadrature we obtained the magnitude of such a vector  $\Delta V = (\sum_{i=1}^3 \Delta v_i^2)^{1/2}$ . Figure 1 shows the spatial distribution of the 32 clusters with calculated  $v_1$ ,  $v_2$ , and  $v_3$  velocity components by adopting the parameters of the disc obtained by [Piatti \(2021a\)](#), see his Table 2). As can be seen, clusters span a wide range of  $\Delta V$  values, that we refer as the residual velocity vector.

By using as residual velocity vector components the values of the dispersion velocity found by [Piatti \(2021a\)](#) (i.e.,

$\Delta v_1=25$  km/s,  $\Delta v_2=50$  km/s,  $\Delta v_3=20$  km/s), we derived the corresponding residual velocity vector magnitude,  $\Delta V = 60$  km/s. We adopted this value to differentiate clusters bound to the SMC rotating disc ( $\Delta V < 60$  km/s) from those scattered by the tidal interaction with the LMC ( $\Delta V > 60$  km/s). With this residual velocity cut, we found 13 clusters with a kinematics that very well match that of a rotating disc, and others 19 whose orbital motions we interpreted have been affected by the effects of tidal forces. Figure 1 depicts their spatial distribution. Clusters with  $\Delta V > 60$  km/s are mainly located in SMC regions projected in the sky that have some previous hints for tidal structures arisen from the interaction between both Magellanic Clouds, namely: a northern branch of the Magellanic Bridge and the Counter-Bridge, which are superimposed at the northeastern outskirts of the SMC; the main Magellanic Bridge, located toward the east from the SMC centre; the West Halo ([Dias & Bekki 2012](#); [Dias et al. 2016](#)) placed at the southwestern end of the SMC disc. This finding confirms our suspicions that kinematically perturbed clusters – those with orbital motions different from those on a rotating disc – accelerated by the LMC gravitational field. Likewise, there are some clusters with  $\Delta V > 60$  km/s that appear projected toward the SMC main body. As far as we are aware, this is the first observational evidence of the distinctive hot kinematics of clusters that depart from the SMC cold disc kinematics. Note that the rotation velocity of the SMC disc is  $25.0 \pm 5.0$  km/s ([Piatti 2021a](#); [Zivick et al. 2020](#)).

Two additional features can be glimpsed at Fig. 1. On the one hand, some clusters with  $\Delta V < 60$  km/s are also projected on the above mentioned SMC tidal structures, which could imply that SMC disc clusters may be projected on galaxy tidal features, in very good agreement with the disc extension out to  $\sim 4$  kpc (see Fig. 1 in [Dias et al. 2021](#)). Therefore, the sole projected cluster position is not enough to straightforwardly identify any clusters as being tidally perturbed. We do not rule out the possible existence of

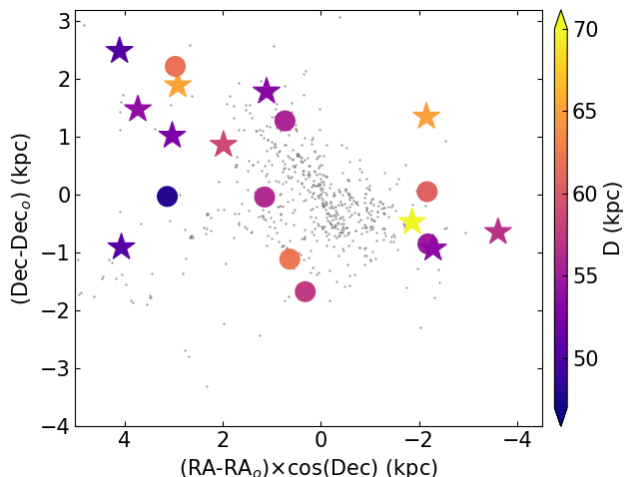


**Figure 2.** Spatial distribution of SMC clusters compiled in [Bica et al. \(2020\)](#) (gray dots). Circles and stars correspond to clusters with residual velocities smaller and larger than 60 km/s, colour-coded according to their heliocentric distances.

cold kinematics clusters in the SMC tidal structures. On the other hand, some clusters with  $\Delta V > 60$  km/s are seen projected on the SMC main body, which could witness the presence of runaway clusters traveling throughout the SMC disc.

In order to disentangle whether there is a possible mixture of kinematically perturbed clusters with  $\Delta V$  smaller and larger than 60 km/s, which would reveal that they would not be easily recognized from their residual velocity vectors, their heliocentric distances are necessary. Unfortunately, there is a small number of clusters with measured distances (see Section 2), which points to the need of observational campaigns in order to build a realistic spatial distribution of them ([Piatti 2021b](#)), and consequently, to trace more precisely the 3D SMC cluster population structure. Previous star cluster studies adopted, in general, a mean SMC distance when dealing with cluster colour-magnitude diagrams ([Piatti 2012, 2014; Piatti et al. 2016](#), and references therein). This is because changes in the distance modulus by an amount equivalent to the average depth of the SMC ([Crowl et al. 2001; Ripepi et al. 2017; Graczyk et al. 2020](#)), so that clusters can be placed in front or behind the SMC, leads to a smaller age difference than that resulting from the isochrones bracketing the observed star cluster features in the colour-magnitude diagram.

With available heliocentric distances for 19 clusters in our sample, we built Fig. 2, which confirms that there is a wide cluster distance range among those projected on SMC tidal structures, in comparison with clusters projected toward the SMC main body. In the northeastern outermost region, there are clusters located in front of the SMC (they belong to the northern branch of the Magellanic Bridge); in the SMC body itself; and behind the galaxy (they are part of the Counter-Bridge) ([Dias et al. 2021](#)). These clusters have very different  $\Delta V$  values as judged by the different symbols used to represent them (circles and stars as in Fig. 1). Similarly, the line-of-sight toward the West Halo also presents clusters placed in front of the SMC; at the SMC distance;

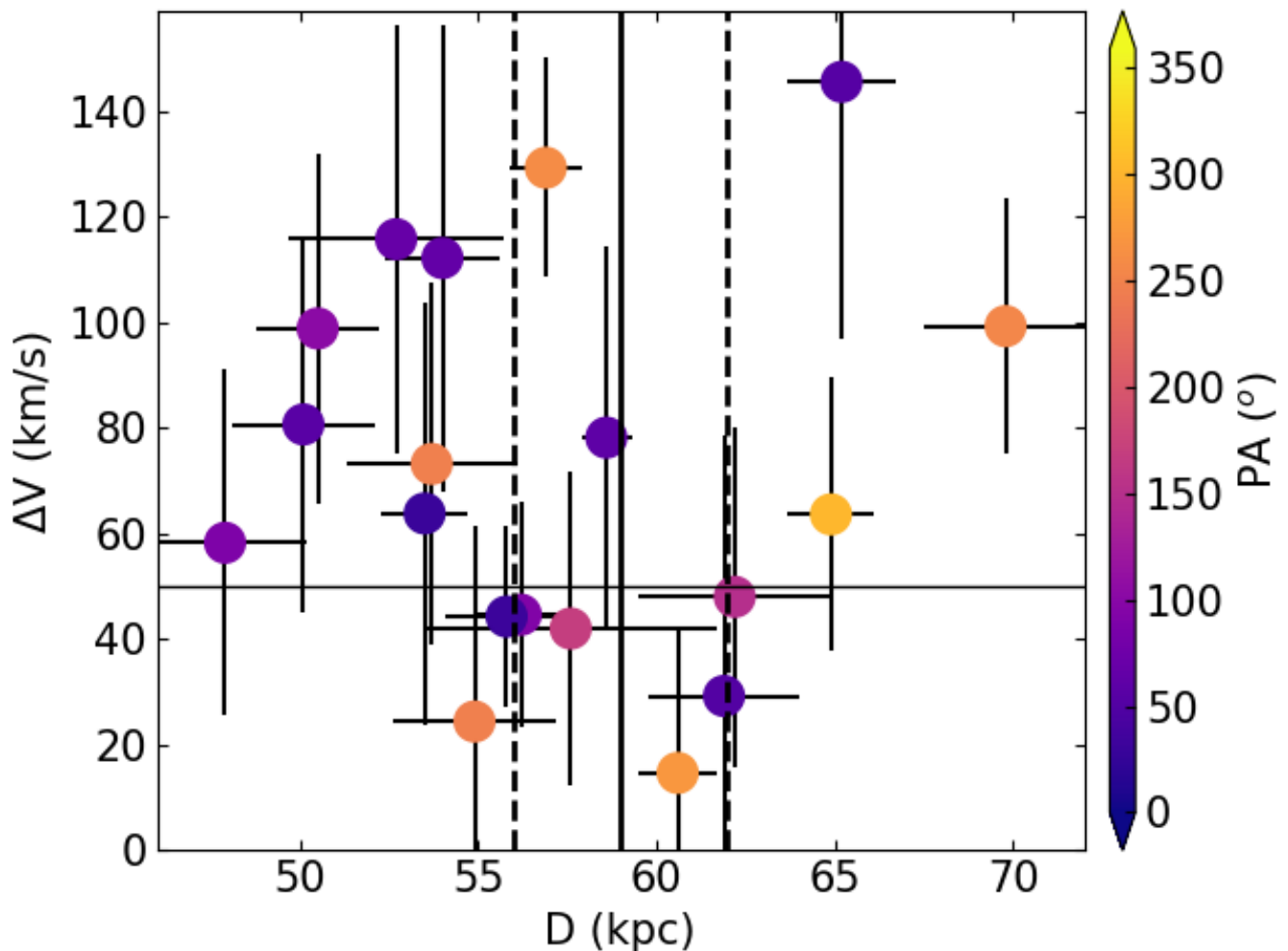
and behind it. This is the first evidence from clusters' distances that the West Halo is a perturbed structure of the SMC, consisting of leading and trailing tails ([Diaz & Bekki 2012; Dias et al. 2016](#)). Nevertheless, in order to determine the extension of both tails, further distance estimates for a larger sample of clusters projected on this sky region are desirable. We also showed that SMC disc clusters ( $\Delta V < 60$  km/s) are spread throughout the whole covered area and located at distances compatible with them being part of the SMC main body ( $56 \lesssim D$  (kpc)  $\lesssim 62$ , [Piatti 2021a](#), and references therein).

Figure 3 reveals a striking distribution of SMC clusters bound to the SMC main body and those pertaining to SMC tidal structures. According to the observed distances of the Magellanic Bridge ( $D < 55$  kpc, [Wagner-Kaiser & Sarajedini 2017; Jacyszyn-Dobrzniecka et al. 2020](#)); of the Counter-Bridge ( $D > 65$  kpc, [Dias et al. 2021](#)); and the present West Halo depth ( $52 \lesssim D$  (kpc)  $\lesssim 70$ ) derived from 5 clusters at PA between  $230^\circ$  and  $270^\circ$ , there is a suggestive residual velocity level at  $\sim 50$  km/s that broadly separates SMC main body clusters from those in tidally induced features. Clusters that belong to these last structures show residual velocities  $\Delta V > 50$  km/s, in very good agreement with the residual velocity cut calculated above (60 km/s) from the SMC dispersion velocities obtained by [Piatti \(2021a\)](#). SMC main body clusters span a wide range of residual velocities, but most of them show  $\Delta V < 50$  km/s, meaning that they have motions similar to the SMC rotating disc kinematics ([Zivick et al. 2020](#)). This outcome shows that the kinematics of SMC tidal structures differentiates from that of its disc.

Among clusters with heliocentric distances smaller than 55 kpc, there are four that belong to the northern branch of the Magellanic Bridge (PA  $< 90^\circ$ ); another one belongs to the main branch of the Magellanic Bridge (PA  $\approx 1^\circ$ ); and one is part of the leading West Halo. All these clusters have  $\Delta V > 50$  km/s. As clusters placed behind the SMC ( $D > 65$  kpc) are considered, there is one that pertains to the Counter-Bridge, and another to the trailing West Halo. They also have  $\Delta V > 50$  km/s. NGC 121 is the oldest known SMC cluster (10.5 Gyr, [Piatti 2011](#)); its location does not coincide with any tidally induced structure ( $((RA-RA_0) \times \cos(Dec), (Dec-Dec_0)) \approx (-2.0$  kpc, 1.3 kpc)), see Fig. 2), but the cluster is at  $D = (64.9 \pm 1.2)$  kpc and has  $\Delta V = 64$  km/s. It is within the kinematic regime of tidally perturbed clusters. The lack of ancient globular clusters in the SMC has been one of the most intriguing enigmas in our understanding of the SMC formation and evolution. [Carpintero et al. \(2013\)](#) modeled the dynamical LMC-SMC interaction and their respective star cluster populations aiming at exploring whether the lack of old SMC globular clusters can be the result of such galaxy tidal interactions. They found that clusters that originally belonged to the SMC are more likely to be found in the outskirts of the LMC or ejected into the intergalactic medium. In this context, NGC 121 could be identified as one of those SMC old escaping clusters.

There are two clusters located at distances compatible with the SMC main body depth whose residual velocity vectors ( $\Delta V > 50$  km/s) suggest that they do not belong to the SMC rotating disc. These clusters are projected toward the northern branch of the Magellanic Cloud and the West Halo, respectively, so that they could either indicate that at the very onset of both tidal structures clusters' kinemat-





**Figure 3.** Residual velocities  $\Delta V$  versus heliocentric distance of SMC clusters. The uncertainties in  $\Delta V$  were calculated using the measured errors in proper motion and radial velocity, and those from the solution for the 3D movement of the SMC centre obtained by Piatti (2021a), propagated through the transformation equations and added in quadrature. Solid and dashed lines represent the SMC centre obtained by Piatti (2021a) and a readily visible SMC main body depth, respectively.

ics change or that they are runaways clusters. We note that other runaway clusters have been identified in the LMC (Piatti et al. 2018). The remaining eight clusters with distance estimates in our sample are SMC main body objects with an SMC rotating disc kinematics ( $\Delta V < 50$  km/s).

For completeness purposes, Fig. 4 illustrates the residual velocity components projected on the Cartesian planes (van der Marel et al. 2002). They witness the stretching experienced by the star cluster population due to tidal effects: those on the northern branch of the Magellanic Bridge roughly moving toward the LMC, while the one observed in the Counter-Bridge traveling in an opposite direction; a picture that is also verified among clusters placed in the closer and farther regions of the West Halo.

In what follows, we mention two different scenarios that could be considered to speculate on possible interpretations of the nature and consequences of the tidal interaction between the LMC and the SMC. They are not exhaustive, but simply introductory, based on recent results.

The gaps and spurs seen in the spatial distribution of

Magellanic Bridge’s clusters (see Fig. 3 in Bica et al. 2020) resemble those observed in tidal tails or streams around Milky Way globular clusters (e.g., Pal 5, GD-1 streams: Grillmair & Dionatos 2006a,b), which have become the most sensitive tracers of the nature and distribution of dark matter in the Milky Way (Bonaca et al. 2019). These tidal tails resulted to be exceedingly cold, with stellar velocity dispersions on the order of 2 km/s or less, and mean motions similar to their parent globular clusters (Price-Whelan et al. 2019). Moreover, the discovery of tidal tails around Milky Way globular clusters using astrometric information usually relies on the assumption that stars in tidal tails share the mean proper motions and radial velocities of globular clusters’ stars (e.g., Carballo-Bello 2019; Sollima 2020; Shipp et al. 2020). The presence of tidal stream substructures extending to hundreds of parsecs around globular clusters also suggest that at least some globular clusters continue to be embedded in dark matter halos (Olszewski et al. 2009; Kuzma et al. 2016). Di Teodoro et al. (2019) studied high-resolution HI data in the SMC and found that out to  $\sim$

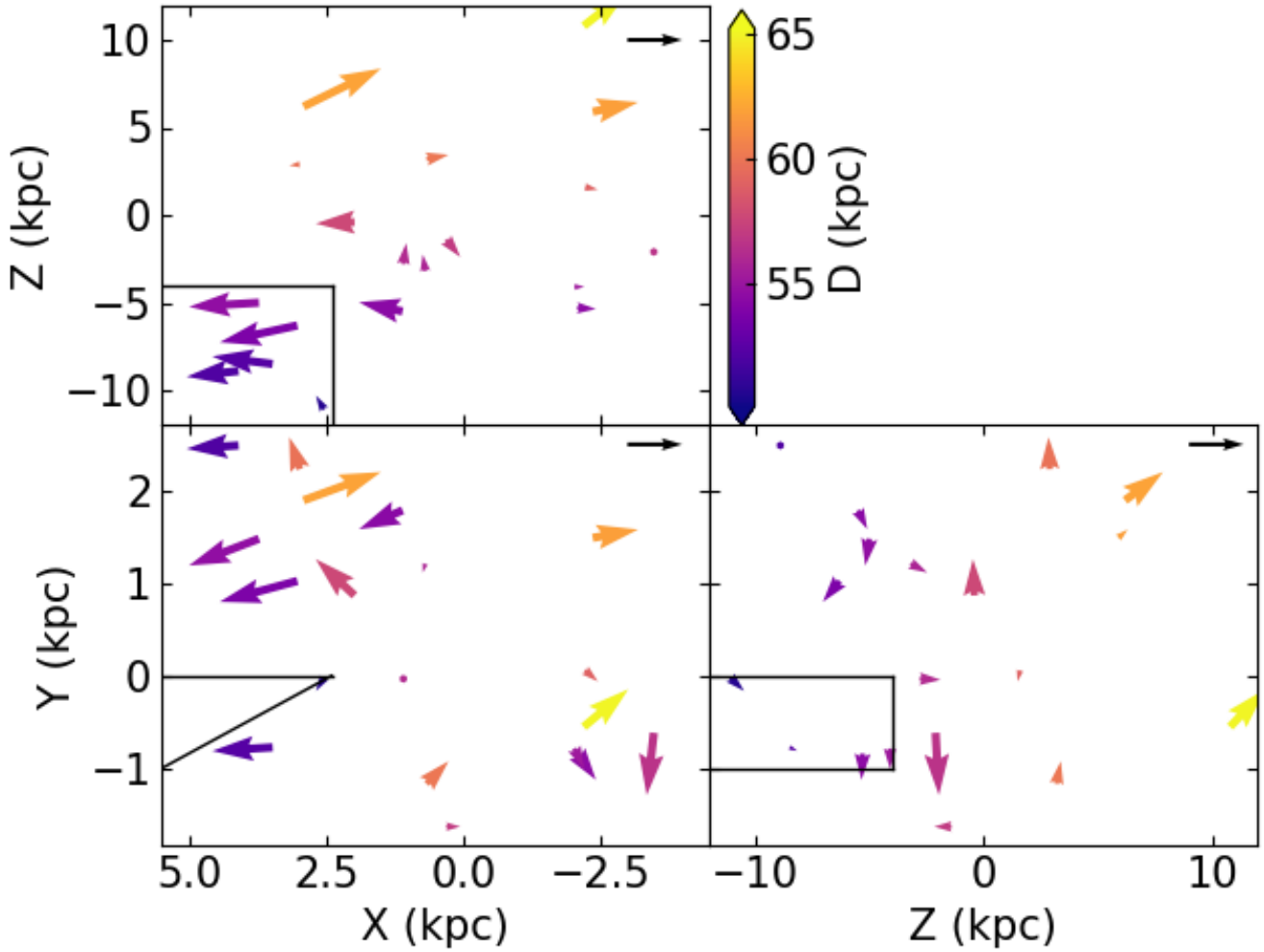


**Figure 4.** Projected spatial distributions of SMC clusters, with the corresponding velocity vectors. The black arrow represents a velocity of  $1\pm\text{km/s}$ . The projection of the Magellanic Bridge is also schematically represented by black lines (Wagner-Kaiser & Sarajedini 2017; Jacyszyn-Dobrzyniecka et al. 2020; Bica et al. 2020).

4 kpc from its centre, the galaxy exhibits a rotating disc kinematics that possibly flattens outwards, despite of the strong gravitational interaction with the LMC. In order to reproduce the observed rotation curve, they argued that a dominant dark matter halo is required. Recently, Koposov et al. (2018) discovered a mildly elliptical ultra-faint dwarf galaxy (Hydrus) located in the Magellanic Bridge with a velocity dispersion of  $2.7\pm 0.5\text{ km/s}$ , which indicates that the system is dark matter dominated.

To the light of our knowledge about the kinematics of globular clusters' tidal tails, the Magellanic Bridge and West Halo do not behave similarly with respect to the SMC. We found that they show motions largely departed from that of the SMC main body (see Fig 3). Therefore, the present observational evidence would be supporting either the notion of a tidal interaction pattern between the LMC and the SMC not comparable to that known for globular clusters and the Milky Way, or that the SMC is not a dark matter dominated dwarf galaxy. We think that Fig. 3 is a suitable starting point to be considered for further investigations on such a debatable conundrum.

#### 4 DATA AVAILABILITY

Data used in this work are available upon request to the author.

#### ACKNOWLEDGEMENTS

I thank the referee for the thorough reading of the manuscript and timely suggestions to improve it.

#### REFERENCES

- Besla G., Kallivayalil N., Hernquist L., van der Marel R. P., Cox T. J., Kereš D., 2012, *MNRAS*, **421**, 2109  
 Besla G., Martínez-Delgado D., van der Marel R. P., Beletsky Y., Seibert M., Schlafly E. F., Grebel E. K., Neyer F., 2016, *ApJ*, **825**, 20  
 Bica E., Westera P., Kerber L. d. O., Dias B., Maia F., Santos João F. C. J., Barbuy B., Oliveira R. A. P., 2020, *AJ*, **159**, 82  
 Bonaca A., Hogg D. W., Price-Whelan A. M., Conroy C., 2019, *ApJ*, **880**, 38

- Bressan A., Marigo P., Girardi L., Salasnich B., Dal Cero C., Rubele S., Nanni A., 2012, *MNRAS*, 427, 127
- Carballo-Bello J. A., 2019, *MNRAS*, 486, 1667
- Carpintero D. D., Gómez F. A., Piatti A. E., 2013, *MNRAS*, 435, L63
- Crowl H. H., Sarajedini A., Piatti A. E., Geisler D., Bica E., Clariá J. J., Santos Jr. J. F. C., 2001, *AJ*, 122, 220
- De Leo M., Carrera R., Noël N. E. D., Read J. I., Erkal D., Gallart C., 2020, *MNRAS*, 495, 98
- Di Teodoro E. M., et al., 2019, *MNRAS*, 483, 392
- Dias B., Kerber L., Barbuy B., Bica E., Ortolani S., 2016, *A&A*, 591, A11
- Dias B., et al., 2021, *A&A*, 647, L9
- Diaz J. D., Bekki K., 2012, *ApJ*, 750, 36
- Dotter A., Chaboyer B., Ferguson J. W., Lee H.-c., Worthey G., Jevremović D., Baron E., 2007, *ApJ*, 666, 403
- Gaia Collaboration et al., 2020, arXiv e-prints, p. [arXiv:2012.01771](https://arxiv.org/abs/2012.01771)
- Glatt K., et al., 2008, *AJ*, 136, 1703
- Graczyk D., et al., 2020, arXiv e-prints, p. [arXiv:2010.08754](https://arxiv.org/abs/2010.08754)
- Grillmair C. J., Dionatos O., 2006a, *ApJ*, 641, L37
- Grillmair C. J., Dionatos O., 2006b, *ApJ*, 643, L17
- Jacyszyn-Dobrzeniecka A. M., et al., 2020, *ApJ*, 889, 26
- Koposov S. E., et al., 2018, *MNRAS*, 479, 5343
- Kuzma P. B., Da Costa G. S., Mackey A. D., Roderick T. A., 2016, *MNRAS*, 461, 3639
- Mackey D., Koposov S., Da Costa G., Belokurov V., Erkal D., Kuzma P., 2018, *ApJ*, 858, L21
- Martínez-Vázquez C. E., Salinas R., Vivas A. K., 2021, *AJ*, 161, 120
- Niederhofer F., et al., 2021, *MNRAS*,
- Olszewski E. W., Saha A., Knezek P., Subramaniam A., de Boer T., Seitzer P., 2009, *AJ*, 138, 1570
- Omkumar A. O., et al., 2021, *MNRAS*, 500, 2757
- Parisi M. C., et al., 2014, *AJ*, 147, 71
- Piatti A. E., 2011, *MNRAS*, 418, L69
- Piatti A. E., 2012, *ApJ*, 756, L32
- Piatti A. E., 2014, *MNRAS*, 445, 2302
- Piatti A. E., 2021a, arXiv e-prints, p. [arXiv:2104.03750](https://arxiv.org/abs/2104.03750)
- Piatti A. E., 2021b, *A&A*, 647, A11
- Piatti A. E., Ivanov V. D., Rubele S., Marconi M., Ripepi V., Cioni M.-R. L., Oliveira J. M., Bekki K., 2016, *MNRAS*, 460, 383
- Piatti A. E., Salinas R., Grebel E. K., 2018, *MNRAS*,
- Piatti A. E., Alfaro E. J., Cantat-Gaudin T., 2019, *MNRAS*, 484, L19
- Pieres A., et al., 2017, *MNRAS*, 468, 1349
- Pietrinferni A., Cassisi S., Salaris M., Castellani F., 2004, *ApJ*, 612, 168
- Price-Whelan A. M., Mateu C., Iorio G., Pearson S., Bonaca A., Belokurov V., 2019, *AJ*, 158, 223
- Ripepi V., et al., 2017, *MNRAS*, 472, 808
- Shipp N., Price-Whelan A. M., Tavangar K., Mateu C., Drlica-Wagner A., 2020, *AJ*, 160, 244
- Sollima A., 2020, *MNRAS*, 495, 2222
- Wagner-Kaiser R., Sarajedini A., 2017, *MNRAS*, 466, 4138
- Zivick P., et al., 2018, *ApJ*, 864, 55
- Zivick P., Kallivayalil N., van der Marel R. P., 2020, arXiv e-prints, p. [arXiv:2011.02525](https://arxiv.org/abs/2011.02525)
- de Vaucouleurs G., Freeman K. C., 1972, *Vistas in Astronomy*, 14, 163
- van der Marel R. P., Alves D. R., Hardy E., Suntzeff N. B., 2002, *AJ*, 124, 2639

This paper has been typeset from a  $\text{\TeX}/\text{\LaTeX}$  file prepared by the author.